ISSN 1846-6168
UDK 669-155.3:539.43+168.2

PONAŠANJE ĆELIJASTE LOTUSNE STRUKTURE KOD ZAMARANJA: NUMERIČKI PRISTUP

FATIGUE BEHAVIOUR OF LOTUS-TYPE POROUS STRUCTURE: NUMERICAL APPROACH

Matjaž Šraml, Janez Kramberger, Sašo Dervarič, Srečko Glodež

Izvorni znanstveni rad

Sažetak: *Cilj ovog članka analizirati je zamornu čvrstoću ćelijaste lotusne strukture crvićastog lijevanog željeza kao osnovnog materijala. Broj ciklusa naprezanja potrebnih za širenje pukotine od inicijalne do kritične dužine pukotine određeno je numerički pomoću modela konačnih elemenata, u okviru Abaqus computation FEM koda. Kriterij maksimalnog vlačnog naprezanja razmatra se kad se analizira putanja pukotine unutar ćelijaste strukture. Izvršenje računalne analize pokazuju kako su koncentracije naprezanja oko individualnih ćelija veće kada vanjsko opterećenje djeluje u transverzalnom smjeru u odnosu na distribuciju ćelija. Članak je produljenje rada, prezentiranog na posljednjoj MATRIB konferenciji u 2014. godini [1]*

Ključne riječi: *numerička analiza, porozne strukture, zamorna čvrstoća*

Original scientific paper

Abstract: *The objective of this paper is to analyse fatigue strength behaviour of lotus-type structure with nodular cast iron as a base material. The number of stress cycles required for crack propagation from initial to the critical crack length is numerically determined using finite element (FE) models, in the frame of Abaqus computation FEM code. The maximum tensile stress (MTS) criterion is considered when analyzing the crack path inside the porous structure. The performed computational analyses show that stress concentrations around individual pores are higher when external loading is acting in transversal direction in respect to the pore distribution. The actual paper is prolongation of the work, presented at the last MATRIB conference in 2014 [1]*

Key words: *Lotus-type porous structures, fatigue strength, numerical analysis.*

1. INTRODUCTION

Lotus-type is a new type of porous material which comprises unidirectional pores. This makes the lotus-type materials very useful for application in lightweight structures, medicine, automotive engineering, sports equipment, etc. [2]. The porosity of lotus metals is usually lower than 70 %, which is lower if compare to some conventional porous metals where porosity is often higher than 70 % [3]. Moreover, pores of lotus-type metals are cylindrical, where the length of pores is usually large if compare to pore diameter (Fig. 1). Since the stress field around the pores depends on the loading direction, the relative high level of anisotropy is typical for lotus-type materials. While uniform stress distribution appears in the case when loading is acting along longitudinal direction of pores, the relative high stress concentration around the pores is characteristic for the perpendicular loading direction.

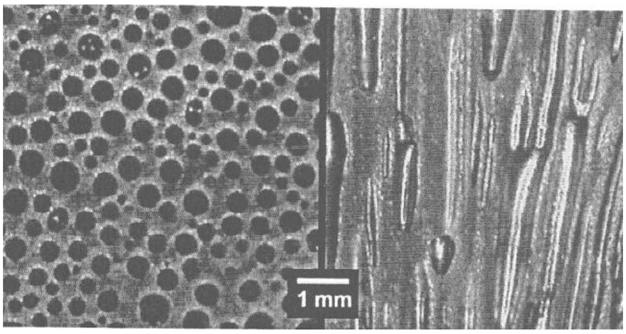

(a) (b)

Figure 1. Cross section of lotus-type porous iron in transversal (a) and longitudinal (b) direction [2].

When porous material is used as a structural element, the fatigue behaviour of such porous structure should be known. Some investigations regarding fatigue behaviour of aluminium porous structures have been reported in [4-6].

However, these results can not be used for lotus-type porous materials due to different pore shapes and their orientations. Seki et al [3, 7, 8] have been studied the fatigue behaviour of cooper and magnesium lotus-type porous structures where the effect of porosity, anisotropic pore structure, and pore size distribution have been taken into account. Their experimental research has shown that for the fatigue loading parallel to the longitudinal axis of pores the stress field in the matrix is homogeneous and slip bands appear all over the specimen surface. This is not the case for transverse loading, where stress field is inhomogeneous and slip bands are formed only around pores because of high stress concentration in this region. Lately, some research works on metal foams have already been done at the University of Maribor [9-11]. However, these materials have not been fully characterized yet, particularly in the way of fatigue life behaviour.

In the present paper, the fatigue process of lotus-type material is divided into the crack initiation and crack propagation phase, where the total service life of treated structural element equals:

$$N = N_\mathrm{i} + N_\mathrm{p}, \tag{1}$$

where N_i is the number of loading cycles required for the fatigue crack initiation and N_p is the number of loading cycles required for the crack propagation from initial to the critical crack length when final fracture can be expected to occur.

When determining the crack initiation phase N_i, the strain life approach with consideration of simplified universal slope method [19] has been used

$$\varepsilon_\mathrm{a} = 0.623 \cdot \left(\frac{R_\mathrm{m}}{E}\right)^{0.832} \cdot (2N_\mathrm{i})^{-0.09} + 0.0196 \cdot (\varepsilon_\mathrm{f})^{0.155} \cdot \left(\frac{R_\mathrm{m}}{E}\right)^{-0.53} \cdot (2N_\mathrm{i})^{-0.56} \tag{2}$$

where ε_a is the total strain amplitude, R_m is the ultimate tensile strength, E is the modulus of elasticity and ε_f is the true fracture strain. It is evident from Eq. (2) that the two exponents are fixed for all metals and that only monotonic material properties R_m, E and ε_f control the fatigue behavior.

The crack propagation phase in this paper is described using Paris equation

$$\frac{\mathrm{d}a}{\mathrm{d}N} = C \cdot \Delta K^m \tag{3}$$

where $\mathrm{d}a/\mathrm{d}N$ is the crack growth rate, ΔK is the stress intensity factor range ($\Delta K = K_\mathrm{max} - K_\mathrm{min}$), and C and m are the material parameters which are determined experimentally according to the load ration $R = K_\mathrm{min}/K_\mathrm{max}$ (the value R=0.1 has been considered in this study). The number of loading cycles N_p required for the crack propagation from initial crack length a_i to the critical crack length a_c can then be determined with integration of Eq. (3):

$$\int_0^N \mathrm{d}N = \frac{1}{C} \int_{a_\mathrm{i}}^{a_\mathrm{c}} \frac{\mathrm{d}a}{\Delta K(a)} \tag{4}$$

2. COMPUTATIONAL MODEL

In publications [2, 11] the regular models with aligned or for some angle aligned pores have been used when determining the strength behavior of lotus-type porous material. In these studies, the used computational models are built of multiple representative volume elements (RVEs) which are presented by a square block with central cylindrical hole of diameter d. The porosity of such structure is then regulated with change of pore diameters by keeping the size of the RVEs as a constant value [2]. In our study, the irregular pores distribution of lotus-type material is considered where only pore distribution in transversal direction is assumed. A special image recognition code was developed, which was used to convert the chosen lotus-type material cross section image into the CAD model which is then used to create the appropriate numerical model. The transverse computational model by square cross section of treated porous structure with length of 3.3 mm and randomly distributed pores with minimum and maximum diameters d_min = 0.084 mm and d_max = 0.47 mm, is introduced, respectively (Fig. 2). For such pores distribution, the porosity is equal to 36 %. The boundary conditions are presented as displacement value of 0.01 mm at the top edge and fixed restraints in the bottom edge of used computational model (Fig. 2).

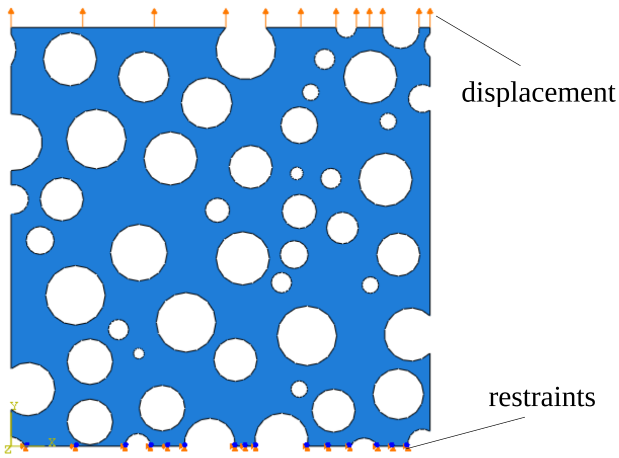

Figure 2. 2D computational model for pores distribution in transversal direction.

In performed computational analyses the lotus-type structure is made of nodular cast iron EN-GJS-400-18-LT as a base material, with monotonic material properties presented in Table 1. The true stress-strain behavior of material (Fig. 3), which is needed for determining the crack initiation phase N_i, is assumed.

Table 1. Monotonic material properties of nodular cast iron EN-GJS-400-18-LT [12]

Yield strength	Ultimate tensile strength	True fracture strain	Modulus of elasticity	Poisson's ratio
R_e [MPa]	R_m [MPa]	ε_f [–]	E [MPa]	ν [–]
256	417	0.235	$1.82 \cdot 10^5$	0.33

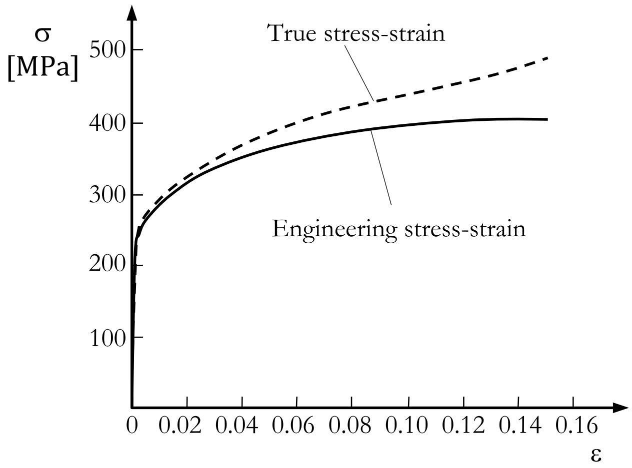

Figure 3. True stress-strain curve of base material [12].

3. NUMERICAL ANALYSIS

Computational models were discretized with quadratic finite elements with linear interpolation. Previous verification of required finite element size has also been done in respect to the results convergence with relative error 0.05. Figure 4 shows the 2D FE-mesh for treated porouos structure.

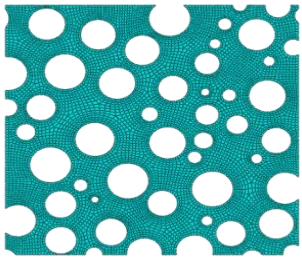

Figure 4. 2D FE-mesh

3.1. Crack initiation phase

When studying the crack initiation phase, the stress filed around individual pores and location of the maximum stress concentration should be determined first. The maximum von Mises equivalent stress $\sigma_M = 350$ MPa with the appropriate total strain $\varepsilon = 0.022$ are recognized in a cross section No. 1 (Fig. 5 (a)). Considering the pulsating loading ($\varepsilon_a = \varepsilon/2 = 0.011$) and material properties as presented in Table 1, the number of loading cycles N_i required for the fatigue crack initiation is then calculated according to Eq. (2). In the next step, the initial crack a_i = 0,05 mm is added into the critical cross section No. 1 (Fig. 5 (b)) and the numerical procedure is continued with the crack propagation phase. When the fatigue crack reaches the critical length, the complete fracture of cross section No. 1 occurs which mean that two neighboring pores are connected with a seam and the complete procedure is repeated regarding to the other critical cross section.

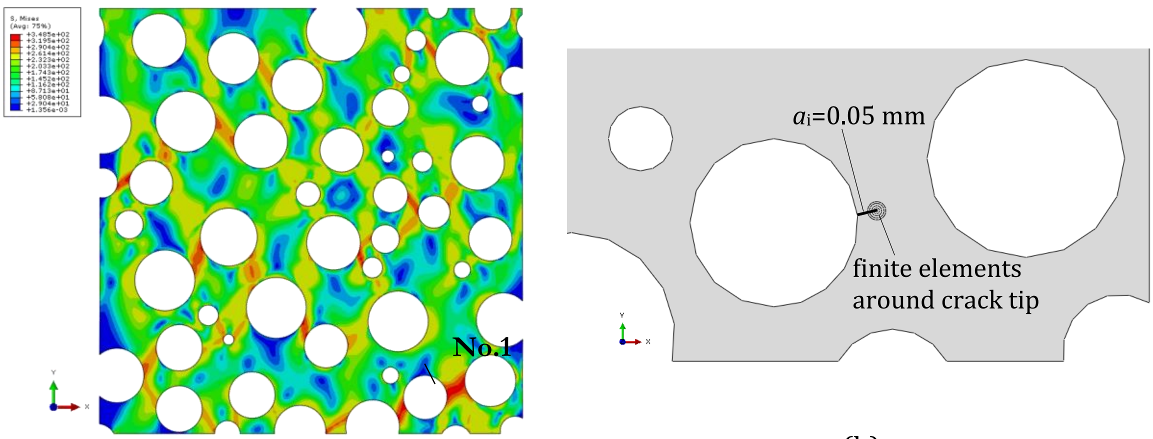

(a) (b)

Figure 5. Crack initiation phase: (a) maximum stress concentration in a cross section No. 1 and (b) initial crack in a cross section No. 1.

3.2. Crack propagation phase

The crack initiation period of each critical cross section is finished with the formation of initial crack of length a_i after the appropriate number of stress cycles N_i. The crack propagation period is then analyzed using Paris equation (3), where the following material parameters have been considered [12]:

$$C = 4.608 \cdot 10^{-12} \frac{\text{m/cycle}}{(\text{MPa}\sqrt{\text{m}})^{3.86}}; \qquad \text{m} = 3.86;$$

$$\Delta K_{\text{th}} = 20.8\ \text{MPa}\sqrt{\text{m}}; \quad \Delta K_{\text{Ic}} = 30.4\ \text{MPa}\sqrt{\text{m}}.$$

Than, the stress intensity factor is determined using Abaqus FEM software, where the equivalent stress intensity range ΔK_{eq} as a combined value of mixed mode conditions ΔK_I and ΔK_{II} has been considered. To analyse the fatigue crack growth under mixed mode conditions the value ΔK in Eq. (3) has to be replaced with the value ΔK_{eq}. The crack propagation angle is in each calculating step determined using maximum tensile stress (MTS) criterion. The analysis of crack propagation has been stopped when the equivalent stress intensity factor range ΔK_{eq} exceeded the critical value ΔK_{Ic} or when the crack reached the vicinity of neighboring pore. At that moment it was assumed that two neighboring pores are connected with a seam and the computational procedure was continued with the crack initiation period in other critical cross section. Figure 6 shows the numerical procedure of crack propagation in a cross section No. 1.

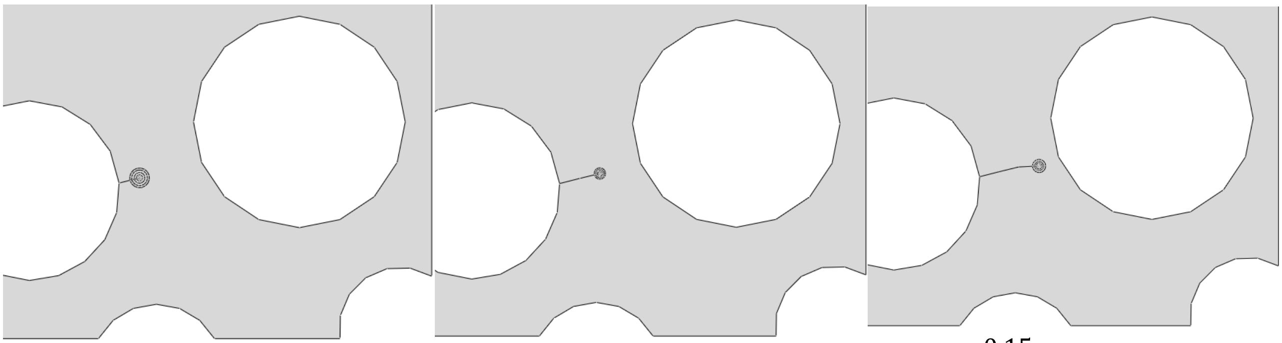

a_i = 0.05 mm
ΔK_{eq} = 15.9 MPa·m$^{0.5}$

a = 0.10 mm
ΔK_{eq} = 20.7 MPa·m$^{0.5}$

a = 0.15 mm
ΔK_{eq} = 27.5 MPa·m$^{0.5}$

Figure 6. Schematic procedure of crack propagation period in a cross section No. 1.

4. DISCUSSION OF THE RESULTS

Figure 7 shows the numbering of critical cross sections where both, crack initiation and crack propagation period have been studied. The maximum stress concentration appeared, firstly, in cross section No. 1 where initial failure occurred after certain number of stress cycles (N_i = 472 cycles for formation of initial crack of length a_i = 0.05 mm and N_p = 212 cycles for this initial crack to propagate until critical length a_c = 0.15 mm). Thereafter, the complete computational procedure is repeated in a cross section No. 2, where the maximum stress concentration occurred in the next calculating step. Here, the seam between neighboring pores in a cross section No. 1 is considered during the numerical analyses. As shown in Figure 7, seven subsequent cross sections have been analyzed in respect to the crack initiation and crack propagation period in treated lotus-type porous structure with pore distribution in transversal loading direction. The final computational results are presented in Tables 2 and 3. The appropriate total number of stress cycles according to Eq. (1) can then be assumed as a total fatigue life of treated structure.

Table 2. Computational results for the crack initiation phase

Cross section No.	Von Mises equivalent stress σ_M [MPa]	Total strain amplitude ε_a	Crack initiation phase N_i [cycles]	Initial crack length a_i [mm]
1	350	0.0110	472	0.05
2	378	0.0229	110	0.03
3	344	0.0136	307	0.03
4	336	0.0121	387	0.03
5	327	0.0108	489	0.03
6	326	0.0200	495	0.03
7	304	0.0090	731	0.03

Table 3. Computational results for the crack propagation phase

Cross section No.	Initial crack length a_i [mm]	Critical crack length a_c [mm]	Function ΔK_{eq} = f(a)	Crack propagation phase N_p [cycles]
1	0.05	0.15	4E+08a^2+35734a+13.171	212
2	0.03	0.09	1E+09a^2+40056a+14.989	113
3	0.03	0.09	1E+09a^2+115195a+6.629	350
4	0.03	0.19	-4E+08a^2+139479a+6.189	1109
5	0.03	0.13	3E+08a^2+113530a+12.203	162
6	0.03	0.13	-5E+08a^2+119507a+10.049	519
7	0.03	0.11	-5E+07a^2+17932a+11.267	1099

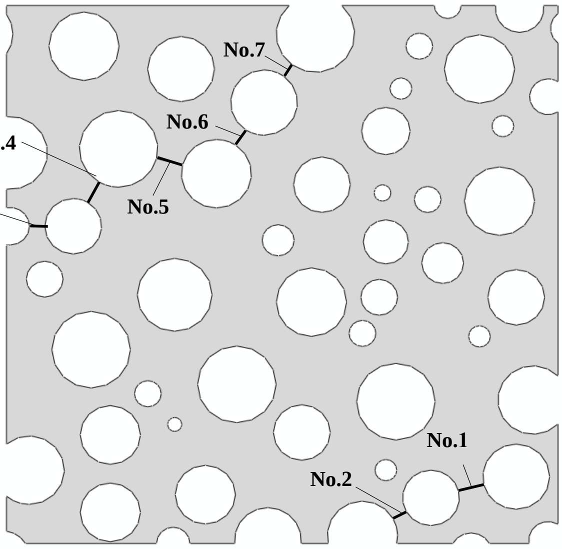

Figure 7. Numbering of critical cross sections.

4. CONCLUSION

The computational fatigue strength investigation in respect to the crack initiation and crack propagation in dynamic loaded lotus-type porous structure made of nodular cast iron is discussed in this paper. The crack initiation period, Ni, has been determined using strain life approach with consideration of simplified universal slope method to determine the number of stress cycles, Ni, required for formation of initial cracks. The crack propagation period, Np, has been determined using Paris equation, where the relationship between the stress intensity factor and crack length has been determined using Abaqus FEM software. Here, the MTS criterion has been considered when analyzing the crack path inside the lotus-type porous structure. The crack initiation and crack propagation period have been studied in seven subsequent critical cross sections between different pores as shown in Figure 7. The total fatigue life, N, of the lotus-type porous structure under given boundary conditions has then been determined as a sum of Ni and Np for all considered cross sections.

Computational results for the pores distribution in the transversal direction have shown that the number of stress cycles for the crack initiation in the individual cross sections varied between 307 and 731, while the number of stress cycles for the crack propagation until final breakage of individual cross section varied between 113 and 1109, which correspond to the regime of low cycle fatigue. Computational results have also shown that quite uniform stress distribution appears in the case when loading is acting along longitudinal direction of pores. Therefore, the appropriate longer fatigue life could be expected in that case.

Acknowledgement: Present research work is financed by the Slovenian Research Agency "ARRS" in the framework of the Research Programme: "Design of porous structures **P2-0063 (B)**".

5. REFERENCES

[1] Kramberger J., Glodež S., Šraml M., Porous material: A Review of fatigue behaviour of metal foams. Zbornik radova = Proceedings. Zagreb: Hrvatsko društvo za materijale i tribologiju, MATRIB 2014, pp. 245-254, (2014).

[2] Vesenjak, M., Kovačič, A., Masakazu, T., Borovinšek, M., Nakajima, H., Ren, Z., Compressive properties of lotus-type porous iron, Computational material science, 65, pp. 37–43, (2012).

[3] Seki, H., Tane, M., Nakajima, H. Fatigue crack initiation and propagation in lotus-type porous copper, Materials transactions, 49, pp. 144–150, (2008).

[4] Amsterdam, E., De Hosson, J.M., Onck, P.R., Failure mechanisms of closed-cell aluminium foam under monotonic and cyclic loading, Acta Mater., 54, pp. 4465–4472, (2006).

[5] Olurin, O.B., McCullough, K.Y.G, Fleck, N.A, Ashby, M,F, Fatigue crack propagation in aluminium’s alloy foams, Int. J. Fatigue, 23, pp. 375–4472, (2001).

[6] Zhou, J., Soboyejo, W. O., An investigation of deformation mechanisms in open cell aluminum foams, Materials Science and Engineering, A386, pp. 118–128, (2004).

[7] Seki, H., Tane, M., Nakajima, H., Effects of Anisotropic Pore Structure and Fiber Texture on Fatigue Properties of Lotus-type Porous Magnesium, J. Mater. Res, 22/11, pp. 3120-3129, (2007).

[8] Seki, H., Tane, M., Otsuka, M., Nakajima, H., Effects of Pore Morphology on Fatigue Strength and Fracture Surface of Lotus-type Porous Copper, J. Mater. Res, 22/7, pp. 1331-1338, (2007).

[9] Vesenjak, M., Borovinšek, M., Fiedler, T., Higa, Y., Ren, Z., Structural characterization of advanced pore morphology (APM) foam elements. Materials letters, 110, pp. 201-203, (2013).

[10] Vesenjak, M., Krstulović-Opara, L., Ren, Z., Characterization of irregular open-cell cellular structure with silicone pore filler, Polymer testing, 32, pp. 1538-1544, (2013).

[11] Vesenjak, M., Ren, Z., Öchsner, A., Dynamic behavior of regular closed-cell porous metals - computational study, International journal of materials engineering innovation, 1, pp. 175-196, (2009).

[12] Čanžar, P., Tonković, Z., Drvar, N., Bakič, A., Kodvanj, J., Sorič, J., Experimental investigation and modelling of fatigue behavior of nodular cast iron for wind turbine applications, Proceedings of EURODYN 2011, Leuven, Belgium, pp. 3252-3257, (2011).

Authors' contact:

izr. prof. dr. Matjaž Šraml
University of Maribor
Faculty of Civil Engineering
Smetanova 17
2000 Maribor
e-mail: sraml.matjaz@uni-mb.si

doc. dr. Janez Kramberger
University of Maribor
Faculty of Mech. Engineering
Smetanova 17
2000 Maribor
e-mail: janez.kramberger@um.si

Sašo Dervarič
University of Maribor
Faculty of Mech. Engineering
Smetanova 17
2000 Maribor

red. prof. dr. Srečko Glodež
University of Maribor
Faculty of Mech. Engineering
Smetanova 17
2000 Maribor
e-mail: srecko.glodez@um.si